Collaborative Research for Future Space Transportation Systems

Oskar J. Haidn, Nikolaus A. Adams, Rolf Radespiel, Thomas Sattelmayer, Wolfgang Schröder, Christian Stemmer, and Bernhard Weigand

Abstract This chapter book summarizes the major achievements of the five topical focus areas, Structural Cooling, Aft-Body Flows, Combustion Chamber, Thrust Nozzle, and Thrust-Chamber Assembly of the Collaborative Research Center (Sonderforschungsbereich) Transregio 40. Obviously, only sample highlights of each of the more than twenty individual projects can be given here and thus the interested reader is invited to read their reports which again are only a summary of the entire achievements and much more information can be found in the referenced publications. The structural cooling focus area included results from experimental as well as numerical research on transpiration cooling of thrust chamber structures as well as film cooling supersonic nozzles. The topics of the aft-body flow group reached from studies of classical flow separation to interaction of rocket plumes with nozzle structures for sub-, trans-, and supersonic conditions both experimentally and numerically. Combustion instabilities, boundary layer heat transfer, injection, mixing and combustion under real gas conditions and in particular the investigation of the impact of trans-critical conditions on propellant jet disintegration and the behavior under trans-critical conditions were the subjects dealt with in the combustion chamber focus area. The thrust nozzle group worked on thermal barrier coatings and life prediction methods, investigated cooling channel flows and paid special attention to the clarification and description of fluid-structure-interaction phenomena I nozzle flows. The main emphasis of the focal area thrust-chamber assembly was combustion and heat

O. J. Haidn (✉) · N. A. Adams · T. Sattelmayer · C. Stemmer
Technical University of Munich, Boltzmannstr. 15, 85748 Garching, Germany
e-mail: Oskar.Haidn@tum.de

R. Radespiel
Technical University of Braunschweig, Hermann-Blenk-Str. 37, 38108 Braunschweig, Germany

W. Schröder
RWTH Aachen University, Wüllnerstraße 5a, 52062 Aachen, Germany

B. Weigand
University of Stuttgart, Pfaffenwaldring 31, 70550 Stuttgart, Germany

transfer investigated in various model combustors, on dual-bell nozzle phenomena and on the definition and design of three demonstrations for which the individual projects have contributed according to their research field.

1 Introduction

Independent access to space has since years been a prerequisite of European policy which required highly reliable and efficient propulsion technologies. In order to remain competitive, Germany, the key developer of combustion devices for liquid propellant rocket engines, initiated a research program more than a decade ago dedicated to increase the theoretical and technological knowledge base of future space-propulsion systems named:

Technological Foundations for the Design of Thermally and Mechanically Highly Loaded Components of Future Space Transportation Systems

The different topics tackled within were based on an assessment of the state-of-the-art of space-propulsion systems. The general findings were: First, the lack of comprehensive fundamental knowledge about design-driving phenomena which required expensive and time-consuming testing at sub- and full scale level of components and systems for any new development. Second, existing engineering design tools base on empirical relations which in order to compensate their uncertainties necessitate sufficient safety factors and result in experience-based posterior optimization procedures. Although the literature provides a lot of information about the different design driving phenomena, the degree of uncertainty and lack of detailed understanding of propellant injection, atomization and mixing, ignition, combustion and its instability, heat transfer and cooling and nozzle flows which define the complexity of liquid propellant rocket engines still exists [1–6]. At this point in time, more than 12 years after the start of the research program, the European space sector is faced with the challenge of *New Space*, where instead of mainly government-sponsored companies which develop and operate launch vehicles an ever increasing number of private start-ups are pushing aggressively into the market. Therefore, the need for new, knowledge-based methods and tools for component design and manufacturing techniques of propulsion technologies which have to be low-cost but still have to meet the requirements of reliability and performance has become even more challenging.

It doesn't surprise that limited resources within SFB TRR40 did not allow to tackle every aspect of cryogenic liquid-propellant thrust chambers in detail. Nevertheless, all major phenomena like propellant injection and mixing including trans-critical phase change thermodynamics, combustion and combustion instability, heat transfer and cooling in thrust chamber processes and nozzles, material and material failure description have been investigated both numerically and experimentally. The strong interdisciplinary character of the program required an appropriate topical structure to identify commonalities and missing links and to coordinate interaction and col-

laboration between the individual research projects within the following research areas:

- A: Structural Cooling
- B: Aft-Body Flows
- C: Combustion Chamber
- D: Thrust Nozzle
- K: Thrust-Chamber Assembly

In each of the three four year funding phases, the program has been focused on different aspects. In the first phase, the main emphasis was put on explorative research aiming at fundamental modeling, development of critical methods and tools and analyses of innovative concepts. The second phase has seen application-focused modeling activities and efforts towards consolidation of technologies, tools and innovations. The final funding phase, the majority of the projects aimed at the establishment of an integrated simulation environment, demonstration of technologies and on hardware demonstration. Hence, the TRR40 collaborative research center was a well-balanced program between fundamental and application oriented research.

2 Research Area A: Structural Cooling

Effective cooling is essential for combustion chambers to keep wall temperatures below material limits. Therefore, the focus of this research area was on foundations and methods for thrust chamber and nozzle-extension cooling. One possible method to sustain such loads are actively cooled ceramic porous structures and combinations of film, transpiration and regenerative cooling. In addition to these subsonic cooling methods, film cooling of rocket nozzles at supersonic conditions were studied both experimentally and numerically. Furthermore, the impact of pressure pulsations on heat transfer and damping performance of resonators was investigated. The general aim of Research Area A was to contribute with models, tools and data to the design or design solutions of the structures for the demonstrator engines defined within Research Area K.

2.1 Transpiration Cooled Ceramic Structures

Utilizing the beneficial properties of highly-conductive ceramics, such a combination could lead to a very effective cooling system for rocket combustion chambers. Multi-scale modeling of transpiration cooling and in particular an appropriate description of the phenomena at the interface between the porous material and the hot gas flow with special emphasis on the coupling conditions has been at the focal point of project A1 (see König et al. in this volume). Interface conditions were designed to couple a hot gas flow, subsonic in a combustion chamber or supersonic in a nozzle, with a porous
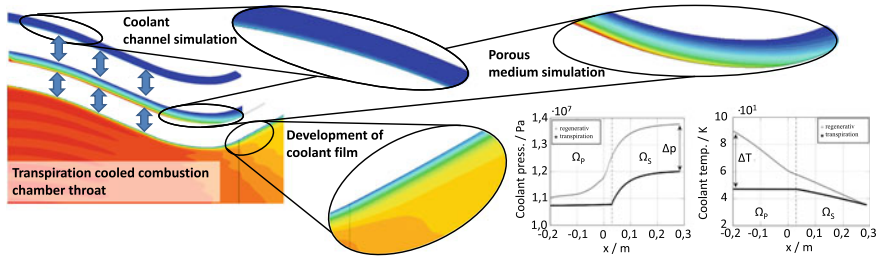
Fig. 1 Temperature distributions for a combined (transpiration, convective, film) cooling concept of a rocket combustion chamber throat area using the developed numerical framework with coupled domains. Relative changes in coolant pressure and temperature to regenerative cooled design (bottom right - Wp - transpiration cooled region, WS - film cooled region)

wall [7] and, more generally, the coupling of two hyperbolic systems in conservation form [8]. Material properties and manufacturing techniques yielded inhomogeneous coolant injection and thus these coupling conditions had to be modified accordingly. Since the modification does not model the interaction of the different scales resulting from the pore size at the surface and the transport of the flow, a more sophisticated approach has been developed based on up-scaling techniques [9]. The idea is to first solve a zeroth-order problem, e.g, a two-domain approach where the hot gas domain and the porous medium were solved alternately using the aforementioned coupling conditions. This information was used to solve cell problems on a micro-scale at the material interface between the hot gas and the porous medium. From the solution of the cell problem, effective coefficients were determined and incorporated into the boundary conditions. Finally, the hot gas flow was solved again using the effective boundary conditions to update the zeroth-order solution. Model reduction strategies have been employed to accelerate solving the numerous cell problems [10]. Figure 1 gives an overview of the flow states in the subsonic and supersonic region of a combustion chamber together with some modeling results.

Parallel to the modeling approach, project A5 (see Peichl et al. in this volume) aimed at the development of lightweight ceramic fiber composites due to their intrinsic favorable thermo-physical properties [11, 12]. The detailed experimental data enable the validation of novel numerical modelling approaches in close cooperation with project A1 including material specific flow conditions [8, 10]. Therefrom, numerical frameworks have been developed to support potential engineering designs in collaboration with project K2 (see Génin et al. in this volume) for rocket applications in combination with classical film and regenerative cooling [10]. All the results were transferred to the design of a Sub-scale Validation Experiment (SVE) with parameters close to applications to be investigated under pressurized hot gas conditions. Figure 2 shows on its left side exit velocities measured with a Pitot probe about 1 mm from the surface and on its right side surface temperatures from a simulation.
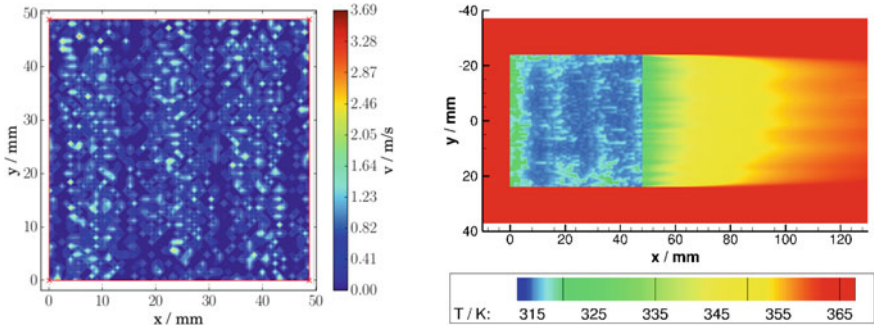
Fig. 2 Measured exit velocities (left)   Simulated surface temperatures (right)
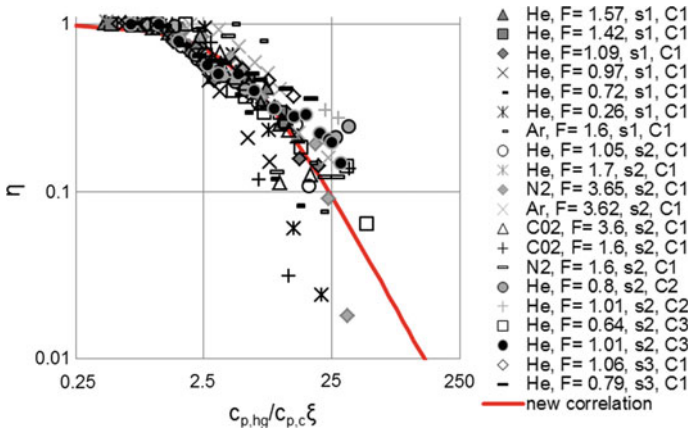

Fig. 3 Correlation of cooling efficiencies gained from experiments with different coolant gases (He, Ar, N2, CO2), different injection slot heights ($s_1 = 0.46$ mm, $s_2 = 0.41$ mm, $s_3 = 0.56$ mm) and different hot gas stagnation conditions (C1: $p_0 = 30$ bar, $T_0 = 3660$ K, C2: $p_0 = 40$ bar, $T_0 = 3685$ K, C3: $p_0 = 50$ bar, $T_0 = 3730$ K), over correlation factor ξ as developed by project A2, enhanced by the ratio of the heat capacities, red curve represents the newly derived correlation

2.2 Supersonic Film Cooling

Project A2 (see Ludescher and Olivier in this volume) aimed at the experimental investigation of supersonic film cooling of a nozzle. Appropriate flow conditions have been provided by a detonation based short-duration facility and validated intensively [13]. A detailed parametric study revealed the impact of different coolant mass fluxes, injection slot heights, hot-gas stagnation conditions and coolant gases on the film cooling efficiency [14]. Based on this data, a new film cooling correlation was developed, see Fig. 3, which can be used as a preliminary design tool for real rocket nozzles. Investigations of the film cooling efficiency in the extension of a dual-bell nozzle indicated that a sharp-edge inflection geometry results in an improved efficiency downstream.
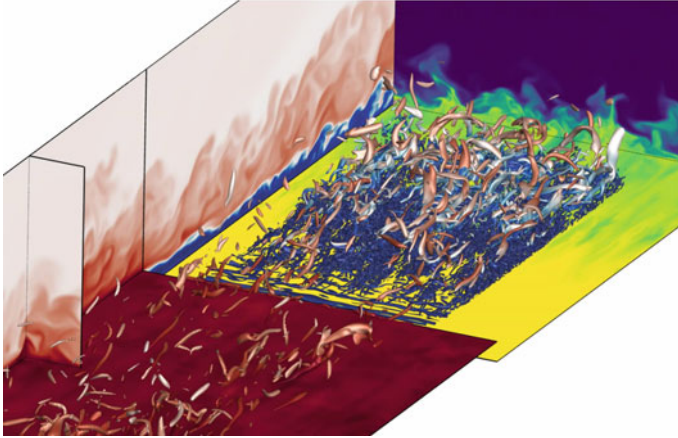
Fig. 4 Snapshot of film-cooling flow field: Vortices colored by the temperature (blue – cold, red – hot), and mass fraction of the cool helium (yellow: 1, blue: zero) on the lower wall and the outlet plane. Flow from lower left

In parallel, project A4 (see Peter and Kloker in this volume), developed a framework to enable high-order direct numerical simulations of film cooling by tangential blowing through a backward-facing step to scrutinize the fundamental thermo-fluid dynamical physics of the cooling/mixing process. A cold laminar supersonic helium flow is fed at various blowing ratios by varying the coolant density into the hot, turbulent flow at Mach 3.3. The cooling effectiveness showed the expected better performance for higher density and thus mass flow rates, also because the laminar/turbulent transition of the film is delayed due to smaller turbulent structures; see Fig. 4 (blowing ratio of one) where transition to turbulence sets in downstream of the step (above the yellow colored wall). Initially, 2D structures (blue) appear near the step that undergo 3D deformation yielding turbulence with structures much finer than the ones in the oncoming hot-gas boundary layer (along the red-colored plane). Injecting a constant mass flow rate is more effective with a smaller slot height; and the coolant Mach number has no significant influence on the flow mixing, as well as the lip thickness. Cooling the wall upstream of the blowing leads to a significantly higher shear and thus to a stronger turbulence production in the free shear layer downstream of the step. Close to the injection slot, the cooling effectiveness therefore shows a reduction compared to an adiabatic upstream wall. Hence, the wall temperature of the oncoming boundary-layer needs to be incorporated for any comprehensive scaling formula used for designing the film cooling. Results of comparisons of tangential to wall-normal helium blowing can be found in [15, 16].

2.3 Damping Performance of Resonators

Within project A3 (see van Buren and Polifke in this volume) an efficient numerical framework to assess resonator performance has been developed which combines
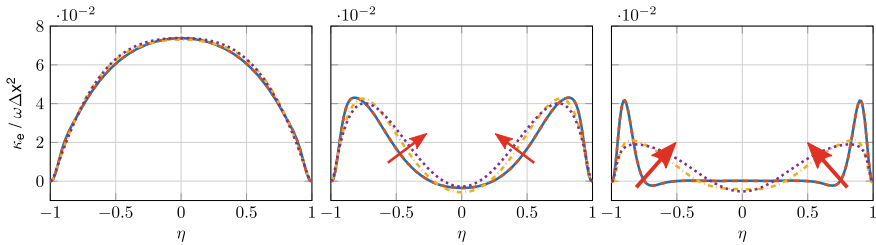
Fig. 5 Local thermal diffusivity over the channel width for increasing Prandtl numbers (left to right). Laminar flows: blue and orange. Turbulent flow: yellow and purple

CFD with a form of supervised machine learning. The acoustic impedance of a resonator was estimated over a wide range of frequencies from time-series data generated in the presence of broad-band excitation. One interesting result was that for a given mean temperature, its spatial distribution within the resonator cavity will influence eigenfrequencies and effective damping of the resonator. The investigation of two fundamental configurations of heat transfer in an oscillating flow revealed that, first, acoustic pulsations enhance the wall-normal heat transfer and, second, if an oscillating resonator flow is characterized by thin hydrodynamic and thermal boundary layers, longitudinal heat transfer increases drastically [17]. Figure 5 physically interprets this finding: Turbulence increases the thermal penetration depth from the wall into the channel (non-dimensional width $-1 \leq \eta \leq 1$). Thus, a wider effective cross-sectional area contributes to the longitudinal thermal diffusivity $\kappa_e/\omega\Delta\omega x^2$.

3   Research Area B: Aft-Body Flows

Turbulent aft-body flows of modern rockets exhibit complex aerodynamic interactions that can lead to significant buffet loads. Furthermore, thermal interactions also can be significant, as aft-body heating is caused by the combined effects of radiation and turbulent transport within a complex flow field. The design of future rocket transport vehicles therefore calls for a thorough understanding of fundamental flow phenomena at the aft-body and its sensitivities with respect to the non-dimensional flow parameters of the outer flow and the propulsive jet.

3.1   Nozzle Flow Separation Studies

Project B6 (see Bolgar et al. in this volume) has contributed to the research area by providing fundamental experimental analyses in transonic and supersonic flow regimes. The experimental set up consisted of generic 2D representations of rocket aft-body flows in a tri-sonic wind tunnel. Sophisticated measurement techniques

Fig. 6 Correlation of wall
pressure fluctuations at x/h =
7 and the vertical velocity
component downstream of a
backward-facing step at
$Ma_\infty = 0.8$
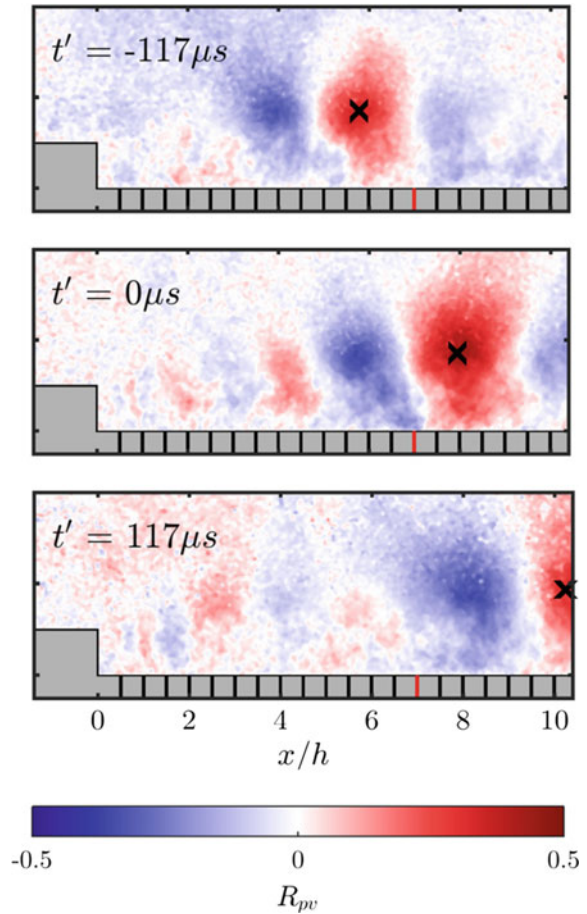
comprised a range of advanced PIV approaches, PSP, and unsteady wall pressure
measurements [18, 19]. Typical research findings for the dynamical flow behavior
are shown in Fig. 6.

3.2 Interaction of Rocket Plume and External Flow

The projects B4 and B1 (see Barklage and Radespiel and Kirchheck et al. in this vol-
ume) both dealt with research into the interactions of a propulsive jet in sub-, trans-,
and supersonic outer flows. Axisymmetric aft-bodies with TIC and Dual-Bell contour
nozzles were investigated in a unique propulsion simulation facility with a supersonic
heated air co-flow and Helium jet flows in order to achieve representative velocity
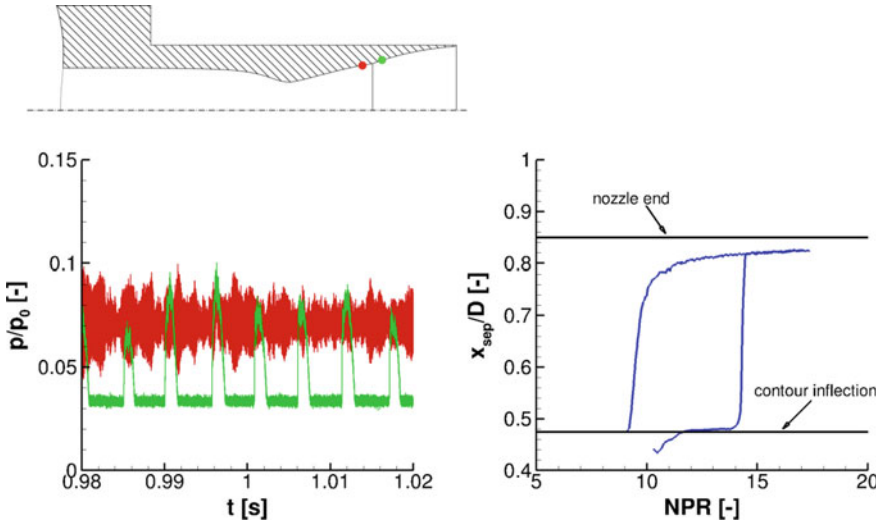ratios were the main objective of project B4 [20]. The aerodynamic integration of

Fig. 7 Pressure signal at the nozzle wall (left) and hysteresis behavior of the separation position inside the nozzle as calculated by LES

Dual Bell nozzles turned out as a particular challenge, as it employs two adaptive design points of operation, the sea-level and altitude modes. The research comprised measurements as well as RANS and LES [21]. Sensitivity studies revealed important effects of nozzle Reynolds number and the aft-body geometry on the transition behavior between the two operation modes. An unstable nozzle operation occurs for certain combinations of these parameters. This features an alternating switching between the two modes leading to high pressure fluctuations in the nozzle, as shown in Fig. 7. As a result, we now have indicators of this unstable mechanism and a parameter space where it occurs. Critical is the interaction with the external-flow shear layer. It was observed that for a reattaching outer flow along the nozzle fairing, unstable nozzle operation occurs while for a non-reattaching flow it does not.

Project B1 entirely focused on the experimental characterization of unsteady aerodynamic and thermal loads at the axisymmetric rocket base along the subsonic to transonic flight trajectory. For simulating the interactions of the hot propulsive jet, a completely new Hot Plume Testing Facility (HPTF) was established in the Vertical Wind Tunnel Cologne (VMK) which duplicated important hot-plume similarity parameters. Gaseous hydrogen and oxygen are fed into the combustion chamber inside the wind tunnel model, see Fig. 8. Unsteady aft-body flow phenomena are identified through high-frequency sensing at the model surface and optical flow-field measurement techniques. Pressure and temperature sensors are used to quantify pressure fluctuations and hot gas entrainment of the recirculating base flow. Non-intrusive optical measurements include high-speed Schlieren Imaging, PIV, and infrared thermography. Access to the measured data is provided by spectral analysis and modal decomposition methods, revealing the characteristic motions of the flow field, which are connected to dominating aerodynamic aft-body loads [24, 25].

Fig. 8 PIV measurement during hot plume interaction test in the VMK
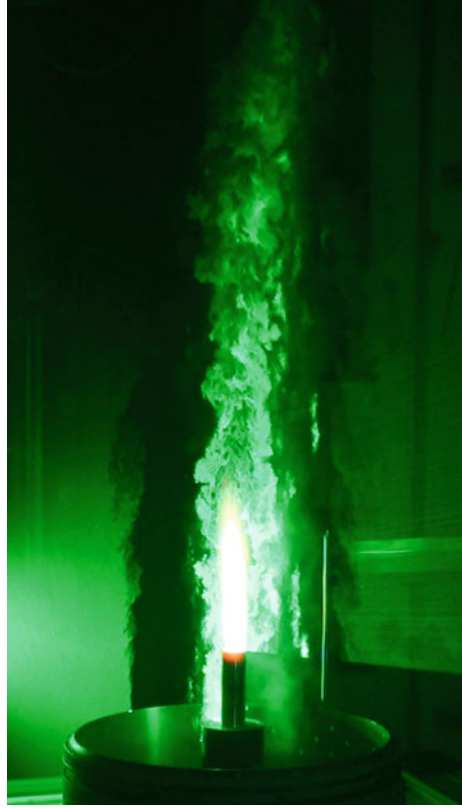
3.3 Modeling of Buffeting

Interaction of mechanical and thermal loads on the nozzle structure were key objectives of projects B3 and B5 (see Loosen et al. and Schumann et al. in this volume, respectively). While B3 concentrated its effort on provision of fundamental knowledge on the origin of buffet loads acting on the nozzle, B5 focused on the flow physics of hot plumes and thermal loads. The B3 team employed high-fidelity scale-resolving simulations and developed flow control means to reduce dynamic loads. Therefore, a large number of configurations including planar geometries, wind-tunnel models with support struts, and axisymmetric flight configurations were analyzed at transonic and supersonic free-stream Mach numbers [22, 23]. The time-resolved numerical simulations of the flow fields were performed with a zonal RANS and LES approach. Extraction of dynamic flow modes yielded understanding of the complex interaction and superposition of periodic and quasi-stochastic flow phenomena responsible for buffet. Figure 9 displays the simulation concept, where RANS equations are solved for the boundary layers attached to the rocket forebody, while aft-body wake flows are represented by LES.
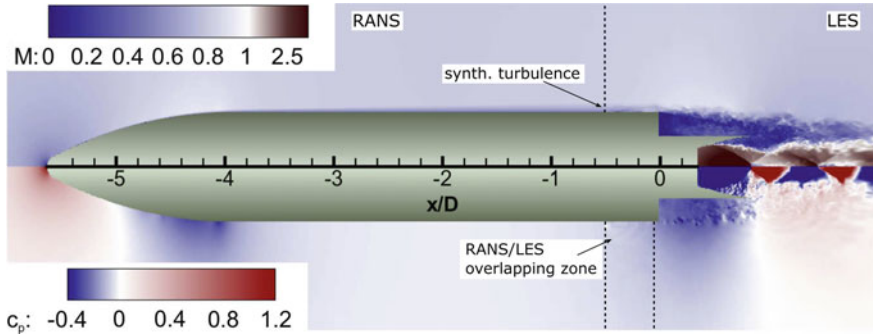
Fig. 9 Instantaneous Mach number and pressure coefficient distribution around a generic configuration representing the flow physics of Ariane 5

The team of project B5 focused on the flow physics of hot plumes and hot walls using numerical simulation [26, 27]. For this purpose, the flow solver was coupled to a thermal structure solver to obtain realistic wall temperature distributions. Scale-resolving hybrid RANS-LES show a surprisingly strong impact of hot plume and hot walls on the aft-body flow. The reattachment of the turbulent shear layer is significantly delayed if a hot plume is present while the temperature in the recirculation region at the base of the launcher is increased. This affects the static pressure distribution along the nozzle fairing and the dynamic loads. While the forces acting on the nozzle structure are very similar for cold and hot plumes assuming cold walls, they change by around 20% due to the hot-wall impact. Figure 10 displays the heated turbulent structures at the base of the launcher as they re-attach to the nozzle fairing and interact with the hot plume.

4 Research Area C: Combustion Chamber

The five projects of Research Area C mainly focused on reacting flows in thrust chambers of liquid-propellant rocket engines (LREs) since they have to operate reliably under extreme conditions, i.e. exceptionally high thermal, mechanical and vibrational loads. This is particularly true for the combustion chamber liner. Near the injector head, oxidizer may get in contact with the hot wall and high temperatures and pressures in combination with near sonic velocities and thin boundary layers imply extreme heat loads further downstream. The projects covered studies of propellant injection, turbulent mixing, combustion and heat release, gas-side heat transfer and thermo-acoustic stability. In addition, several novel simulation tools for these processes have been developed, which have significantly advanced the state-of-the-art in LRE modelling.
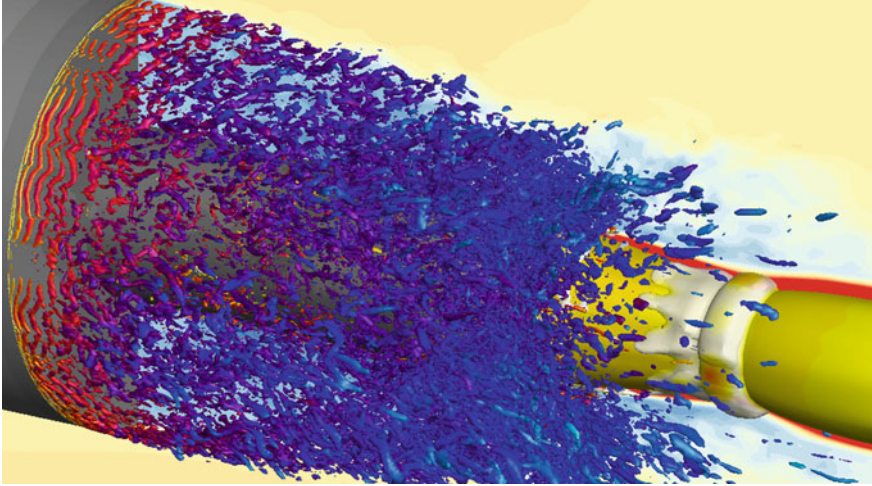
Fig. 10 Free shear layer enclosing the recirculation region of the generic rocket base and the hot plume at transonic flow conditions in VMK

4.1 Dynamic Processes in Trans-Critical Jets

Project C4 (see Föll et al. in this volume) provided a framework to perform jet disintegration experiments under well-defined conditions, in order to gain a better understanding of the physics at high pressures. This provides the starting point enabling the validation of the different thermodynamic models employed in other projects of the research area. Figure 11 schematically shows the different high-pressure disintegration regimes that were obtained by varying the injection temperature across the critical temperature of the fuel (i.e., $0.8 < T_{inj}/T_c < 1.2$). As can be seen, the jet morphology varies drastically across the disintegration regimes and requires the development of accurate thermodynamic models capable of describing both non-equilibrium phase transitions and multi-component mixing processes in dense gases [28].

After the phenomenological classification of the disintegration regimes, the experimental activities were mainly focused on the acquisition of quantitative data to characterize the mixing process in high pressure super-critical jets. For this purpose, the applicability of Laser Induced Thermo Acoustics (LITA) was extended to high pressure turbulent jets. The LITA data show that the adiabatic mixing assumption, commonly employed in many solvers, loses its validity even at Reynolds numbers as high as 10^5, in presence of large temperature and concentration gradients. This required the development of more accurate models for the description of diffusive transport on the mixing process. The numerical and theoretical activities focused on the implementation and assessment of thermodynamic and phase transition models and aimed at providing an accurate description of the mixing process in trans-critical jets. For that purpose, a novel numerical framework based on a high order discontinu-
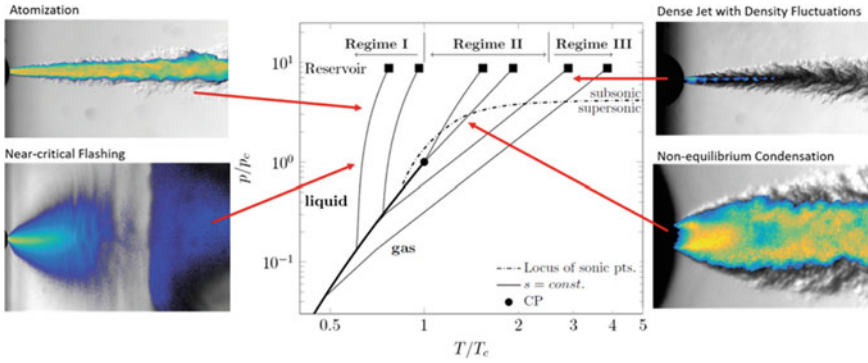
Fig. 11 Schematic overview of the different disintegration regimes with increasing injection temperature

ous Galerkin approximation was developed by extending the open-source large eddy simulation code FLEXI to the multi-phase regime. High-order accuracy in combination with local refinement and robust shock-capturing allows high resolution of the multi-scale phenomena around the critical point. Real-gas effects are handled accurately and efficiently by means of adaptive tabulation techniques. The numerical modelling of the jet-mixing process turned out to be a difficult process that strongly depends on the numerical diffusion of the numerical simulation also. Therefore, a central aspect was to study different approaches to assess, which models adhere best to the experimental findings. The knowledge about the consistency between experimental data, thermodynamic theory and the prediction provides a prerequisite for the correct calculation of such processes in the framework of thrust-chamber flow computations.

4.2 Injection, Mixing and Combustion Under Real-Gas Conditions

For the numerical investigation of injection, mixing and combustion under LRE conditions, a CFD tool has been developed within project C1 (see Traxinger et al. in this volume) which employs the open-source toolbox OpenFOAM [29]. The particular focus was on the thermodynamics of combustion modelling under high-pressure conditions (Fig. 12). For the accurate representation, a fully consistent framework based on a cubic equation of state was devised considering real-gas and phase separation effects [30]. Several combustion models have been implemented ranging from tabulated combustion models for real-gas and non-adiabatic conditions up to transported PDF approaches [31]. Applying this framework, different LES investigations have been conducted: For inert and reacting cases, detailed thermodynamic studies [30–32] showed the occurrence of single-phase instabilities. Under LRE-like conditions, this phase separation processes can be attributed to mixing, i.e., to the
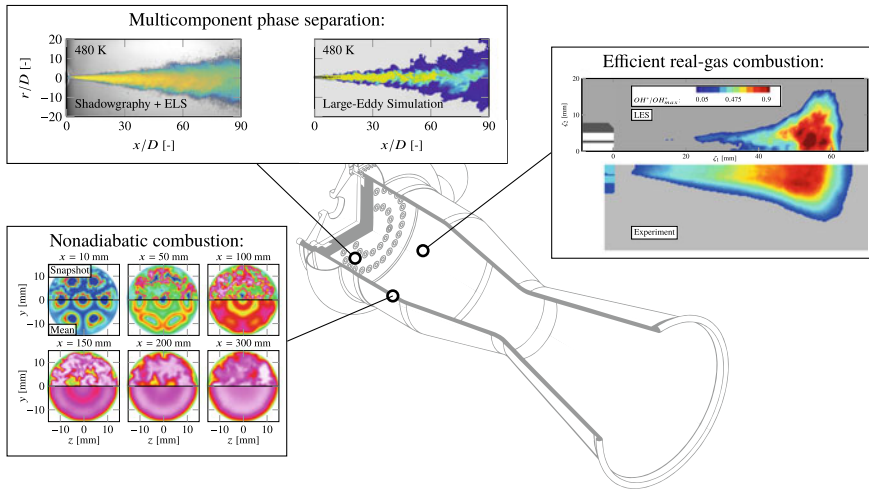
Fig. 12 Critical point and real gas effects on non-adiabatic reacting flow

thermodynamic behaviour of the multi-component system. For the investigation of the combustion process in LREs and the reliable prediction of wall-heat fluxes, a numerical simulations [33] of a multi-element combustion chamber has been conducted. The comparison with experimental data showed good agreement and wall-modeled LES together with a non-adiabatic tabulated combustion model has been deduced as a promising candidate for accurate, reliable and efficient numerical simulations. Thereby, heat losses and associated influences on the reaction kinetics can be considered. In conclusion, the developed CFD code is well-suited for the numerical investigation and reliable prediction of the injection and combustion process under LRE conditions.

4.3 Boundary Layer Heat Transfer Modelling

The aim of project C6 (see Olmeda et al. in this volume) was to model wall heat transfer in LREs with high accuracy and to investigate the influence of wall films on cooling. OpenFoam [29] has been used to carry out the combustion simulations. Flamelet tables have been generated in a pre-processing phase taking into account the influence of non-adiabatic sources and turbulent fluctuations since the conventional adiabatic models are not able to capture the recombination phenomena in proximity of the cooled chamber walls. Large-Eddy Simulations with and without film cooling have been performed, achieving good agreement for the wall heat flux with the experimental data [34]. The heat flux is decreased by the cooling film, the full mixing of fuel and oxidizer is reached in the same position in the axial direction as for the
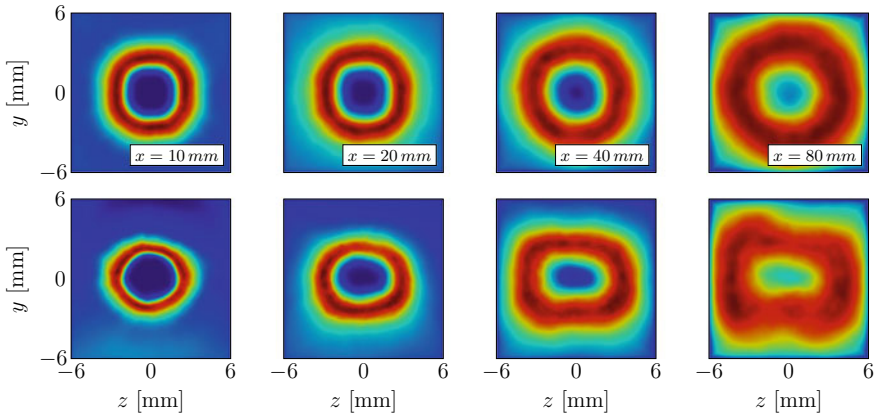
Fig. 13 Temperature field at cross sections x = 10, 20, 40, 80 mm. Top: without film. Bottom: with film

non-cooled case. The injected film increases the chamber pressure after the inlet with respect to the non-cooled setup. The cooling film causes a drop of the flame thickness perpendicularly to the film direction. The cooling effect of the film ceases to be effective after half the length of the combustion chamber (Fig. 13).

The code CATUM [35] has been used to analyze the effect of wall roughness on the velocity and temperature fields, which causes an enhancement of the heat transfer at the wall. Different roughness models have been implemented and tested. The results have shown good agreement with the DNS data available [36], particularly considering the low transitionally rough regime.

4.4 Combustion Stability of Rocket Engines

Projects C3 and C7 (see Chemnitz and Sattelmayer and Armbruster et al. in this volume, respectively) were focused on combustion instabilities. While C3 aimed at the numerical assessment of the stability of the reacting flow focusing on efficient models suitable for industrial design processes, C7 concentrated on establishing a data base on forced and intrinsic instabilities in a LOX/GH2 model rocket engine. To fulfill the demand for a lean tool, a hybrid approach relying on the linearized Euler Equations (LEE) was chosen. A quasi one-dimensional flow was used as reference state for the perturbation analysis to avoid the computationally cost-intensive resolution of the large number of diffusion flames typically present in combustion chambers of larger engines. As the combustor acoustics may be severely influenced by other thrust chamber components, these were included as well via frequency dependent boundary conditions. An approach to quantify the flame feedback from Flame Transfer Functions (FTF) obtained from single-flame simulations using source terms was
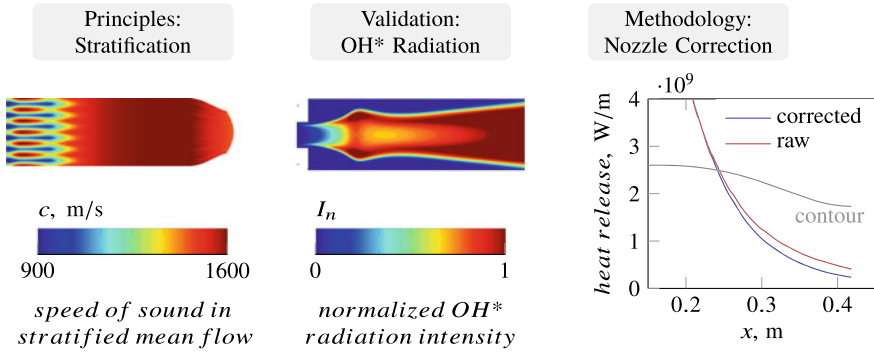
Principles: Stratification	Validation: OH* Radiation	Methodology: Nozzle Correction

c, m/s

900 — 1600

speed of sound in stratified mean flow

I_n

0 — 1

normalized OH* radiation intensity

heat release, W/m

$\cdot 10^9$

corrected
raw

contour

x, m

Fig. 14 Numerical assessment of thermo-acoustic stability of LREs

later enlarged and combined with chamber acoustics to replace the LEE calculations in time domain by an eigenvalue analysis in frequency space [37, 38]. The approach was validated using the stability data from the C7 project.

Additionally, a procedure for calculating mean flow fields that are fully consistent with the Euler Equations has been introduced. Based on this approach, the impact of the diffusion flame structures in the chamber flow (see Fig. 14: Principles) on the acoustics has been studied [39]. The acoustic mode and the oscillation frequencies have been found to be insensitive to radial stratification. The associated damping rates changed stronger due to their dependence on the entropy and vorticity modes. The results were used for the adaption of the FTF calculation method. To further validate the single flame simulations, an efficient method for the calculation of OH* radiation has been developed (see Fig. 14: Validation). For the acoustic characterization of the virtual thrust chamber demonstrators, the mean-flow calculation procedure was extended to account for the respective chamber geometry (see Fig. 14: Methodology). Based on previous studies on the impact of dampers on rocket engine acoustics [40], the relation between mode split and absorber characteristics was identified [41]. This allows to specify constraints for the absorber characteristics that can be used to design a damping device without explicitly re-evaluating the chamber acoustics.

The hot-fire tests were conducted at the P8 test bench. One combustor, BKD, runs with the cryogenic propellants LOX/H_2 injected through 42 shear-coaxial injectors and operates at supercritical pressures for oxygen. Gröning was able to prove that self-excited combustion instabilities of the 1 T mode in the BKD are driven by injection-coupling through acoustic eigenmodes in the LOX injector [42]. This type of coupling mechanism is rather common for cryogenic rocket engines with coaxial injectors [2]. A water-cooled measurement ring including a small sapphire window was designed and installed in BKD. Simultaneous high-speed imaging of OH* and also blue radiation (BR) was conducted with 60,000 FPS. Mean flame images for the operating condition of $p_{cc} \approx 80$ bar and ROF 5.3 are shown in Fig. 15. The thin shear layer originating from the injector exit is rapidly spreading along the reaction
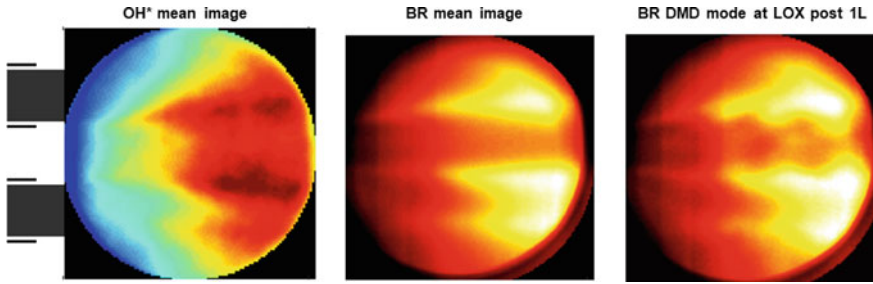
Fig. 15 Time-averaged OH* image (left) and blue radiation image (middle), and reconstructed DMD mode at the injector resonance frequency (right). All images are in false colour

zone in downstream direction, as can be seen in the OH* image (left) and in the BR image (middle) as well. The path of the LOX jet is visible in the BR image only.

The flame dynamics were investigated by Dynamic Mode Decomposition (DMD). The influence of the 1 L resonance in the LOX injector on the LOX jet is visualized on the right side in Fig. 15. Standing waves in the injectors lead to periodic variation of the injected LOX mass flow rate, producing wavy structures on the surface of the dense LOX jet. The symmetrical character of the LOX jet pulsation is consistent with a periodic variation in the rate of injection [43, 44]. Therefore, the LOX jet dynamics found in the experiments is in agreement with the LOX injector coupling mechanism hypothesized by Gröning [42]. Since such detailed flame visualization has not been achieved previously under representative conditions, this data will be of high value for the future validation of numerical simulations and predictive tools.

5   Research Area D: Thrust Nozzle

Thrust nozzles are a highly critical and extremely loaded propulsion component of any space transportation system. Designed for the enormous thrust forces in the axial direction, they have to withstand radially, and temporally fluctuating loads as well. Moreover, the nozzles very often are the major means for thrust vector control. Due to its nominal load, the thrust nozzle is designed as a thin-wall structure. For primary propulsion systems, it consists of actively cooled metallic material more or less exclusively. The nozzle flow is determined by the flow state at the outlet of the combustion chamber which defines the outlet conditions and the downstream boundary conditions at the nozzle exit. The latter vary along the ascent trajectory and strongly interact with the unsteady base flow, i.e., the flow field near the aft face of the main body of the rocket. Especially during engine start-up and the early ascent phase, the internal nozzle flow is dominated by shock induced unsteady separations which result in pronounced fluctuating asymmetric radial pressure loads, so-called side loads, and local peaks in the heat load distribution. These local and tempo-
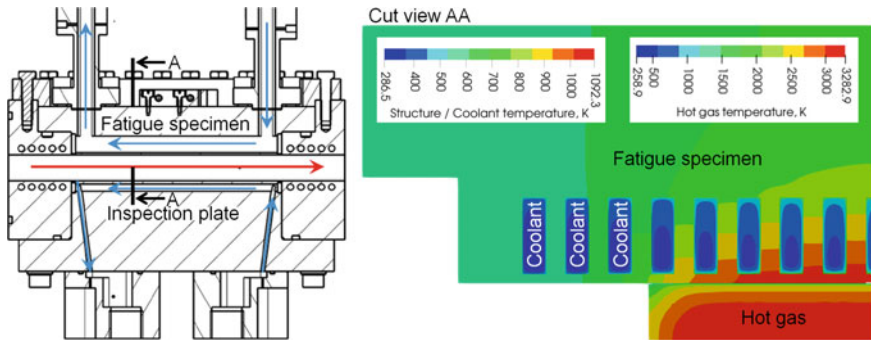
Fig. 16 Fatigue Segment developed for Cyclic Life Determination

ral inhomogeneities which interact with the nozzle structure are the key drivers for thrust-nozzle design and thus were in the focus of Research Area D. The six projects of research area D dealt with the physical fundamentals and modeling of the mechanical and thermal fluid-structure interaction in the thrust nozzle. New concepts and methods were developed to master those fluid-structure interactions. The following discussion covers only an excerpt of the findings. A more thorough analysis of the results is given in the contribution of each project.

5.1 Thermal Barrier Coatings and Component Life Prediction

Methods and models for nozzle lifetime prediction and measures to extend the overall lifetime of rocket engines were developed by considering the impact of thermal and mechanical loads. The tools comprising the thermo-mechanical material modelling, e.g., for metallic alloy and CMC material, and the fluid-structure interaction derived in project D3 (see Barfusz et al. in this volume) were validated on the basis of the sub-scale combustion chamber experiments performed in project D9 (see Hötte et al. in this volume). There, a fatigue segment, see Fig. 16, was placed sufficiently downstream in a GOX/GCH4 combustion chamber with rectangular cross section to guarantee fully developed hot gas conditions and as such allow for a proper determination of the cyclic life of such structures. The fatigue segment housed an actively cooled fatigue specimen made of CuCr1Zr and was equipped with an extensive measurement technique. The specimen was loaded cyclically and inspected regularly for deformations, roughness, and leakages. A load cycle consisted of pre-cooling, hot gas run and post-cooling phase. The results showed that the height of the deformation profile increased nearly linearly with the number of load cycles until the cooling channel structure failed due to the so-called doghouse effect, see Fig. 17.
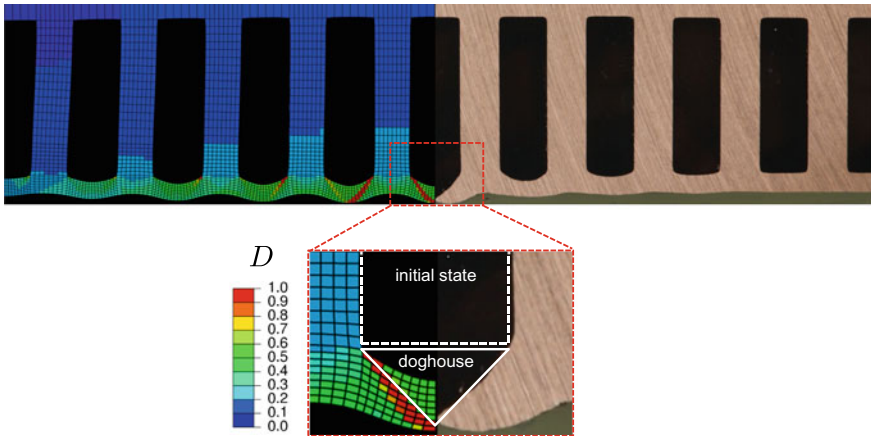
Fig. 17 Comparison with experimental observations - deformed geometry and damage contour after 47 cycles obtained from simulation (top) and cut view of the fatigue experiment after 48 cycles showing a macroscopic crack in the center cooling channel (bottom)

While the slope of this deformation profile strongly depended on the thermal loads, i.e., temperature level and temperature gradients, the critical deformation which occurs in case of failure was not affected. For lifetime prediction, the temperature determined from the conjugate heat transfer (CHT) served as input for a series of quasi-static mechanical analyses, in which a newly developed visco-plastic damage model was utilized [45, 46]. During the numerical analysis of the deformation process, it was found that the damage initially spread diagonally from the cooling channel corner to the hot gas wall and eventually merged into a macroscopic failure zone. The comparison with the experiment, which is shown in Fig. 17, revealed that the number of cycles until failure, the position of maximum deformation and degradation, and the final failure mode, i.e., the doghouse effect, were accurately predicted by the simulation. To protect the copper liners of liquid-fuel rocket combustion chambers against the doghouse effect, a new metallic coating system was developed in project D2 (see Fiedler et al. in this volume), consisting of a NiCuCrAl bond-coat and a Rene 80 top-coat, and applied with high velocity oxyfuel spray (HVOF). The coatings were tested in laser-cycling experiments to investigate their performance under large heat-fluxes and thermo-shock loading. FEM simulations were used to identify critical loads for coating failure to develop guidelines for coating design [47, 48]. Delamination, buckling, and diffusion pores can be avoided by following these new guidelines for coating design, vertical cracks, see Fig. 18, however, are inevitable for any coatings in the combustion chamber. The cracks can be tolerated in rocket-engine application as they close at high temperature and are not expected to propagate into the substrate.
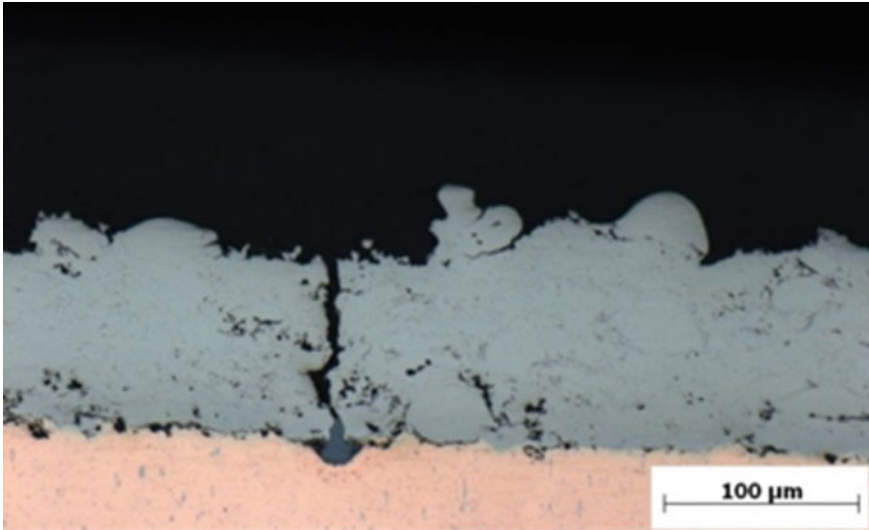
Vertikal Crack

Fig. 18 Vertical crack in a thermal barrier coating

5.2 Cooling Channel Flows

The heat transfer through cooling ducts was investigated in projects D4 (see Kaller et al. in this volume) and project D9 (see Hötte et al. in this volume) experimentally and numerically. Based on the reference experiment [49], the flow field in the thermal entrance region of a straight high aspect-ratio water-cooling duct with an aspect ratio $AR = 4.3$, a Reynolds number of $Re_b = 1.1 \times 10^5$ and an average Nusselt number of $Nu = 371$ was investigated by LES and RANS simulations. The validation of the LES with DNS data and the good agreement between numerical LES and experimental PIV results for velocity and Reynolds stress profiles are reported in [50]. Figure 19 depicts the temperature and secondary flow development along the heated domain in the lower duct quarter. The secondary flow increases the mixing of hot and cold fluid. The overall temperature increase is relatively moderate. The comparison of the RANS and LES data shows the deviation to increase with rising flow complexity.

5.3 Fluid Structure Interaction

Thermo-mechanical loads caused by high-enthalpy flows in conjunction with constraints on the movement of the structure lead to undesirable localized deformation and buckling phenomena. Experimental studies of the heat transfer under super-
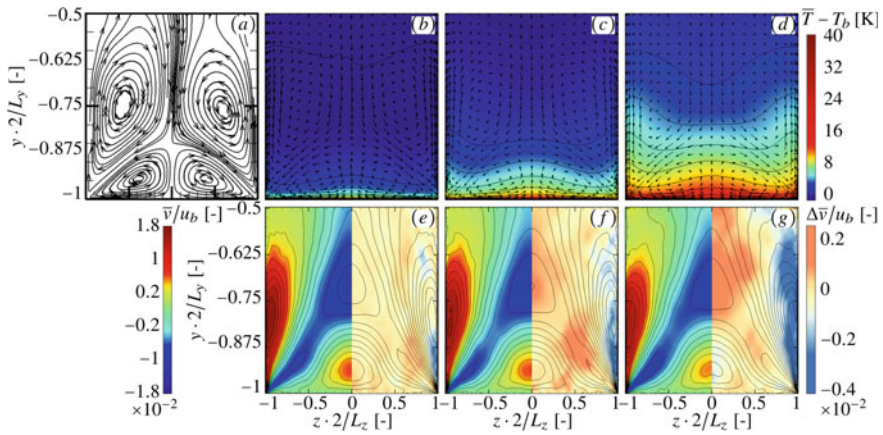
Fig. 19 Corner vortices, temperature profile development and accompanying secondary-flow change represented by the lower wall-normal velocity. The figure shows the lower duct quarter at streamwise positions of 50, 200, and 600 mm (from left to right). In the bottom row, the left half of each picture shows v and the right the v-change with respect to the adiabatic case

sonic conditions including thermally-induced deformations and their interaction with the flow field were conducted in project D6 (see Daub et al. in this volume). The fluid-structure interaction (FSI) experiments were performed in a very high-temperature environment such that massive deformations with and without plastic behavior occurred [51]. The additional numerical flow analysis was part of a coupled fluid-structure interaction simulation conducted in project D10 (see Martin et al. in this volume). The FSI modeling was carried out by an iterative staggered scheme. For the mechanical structural computation, a thermodynamic consistent elasto-viscoplastic material model with thermal expansion for large deformations was developed and implemented into a user material subroutine in Abaqus. Figure 20 emphasizes the detached bow chock, the evident deformation of the panel, and the drastic temperature increase on the deformed surface.

6 Research Area K: Thrust-Chamber Assembly

The major task of this research area with the topics combustion and heat transfer, Dual-Bell nozzle flows and thrust-chamber demonstrators was on maturing and transfer of innovative concepts, solution methods and design tools towards industrial application.

Projects K1 (see Perakis and Haidn in this volume) and C5 (see Seitz et al. in this volume) were dedicated to establish a broad base of experimental data applying different model combustors operating with gaseous as well as liquid propellants. They developed and applied different numerical models capable to predict typical
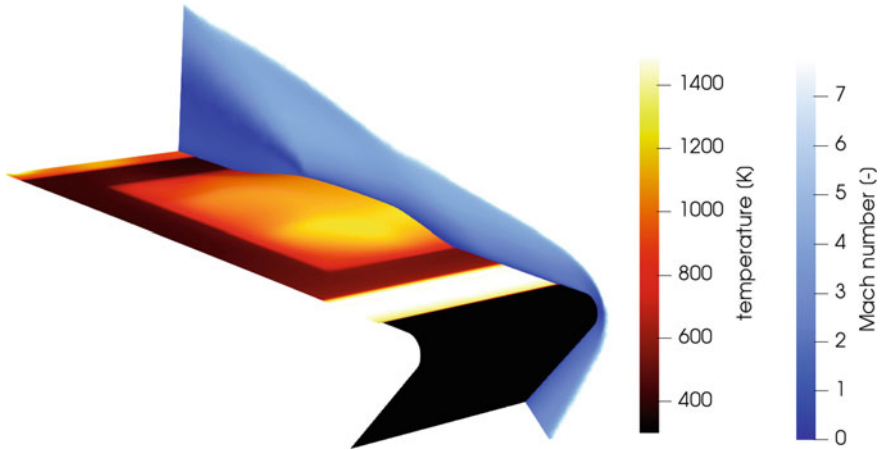
Fig. 20 Numerical fluid-structure interaction analysis of the buckling phenomenon

processes in rocket engines using this data base with sufficient accuracy. Project K2 (see Génin et al. in this volume) aimed at providing both an experimental data base as well as numerical tools for sub-scale dual bell nozzles operating in cold and hot-gas mode. Project K4 (see Eiringhaus et al. in this volume) led by the industrial partner ArianeGroup, defined three virtual thrust-chamber demonstrators that reflected all main characteristics of current European upper and main stage engines. Additionally, they incorporated advanced features like e.g. transpiration cooling, dual-bell nozzle extensions or heat-transfer enhancement methods for expander-cycle engines. Thereby, these virtual demonstrators included all topics addressed by the different projects within TRR 40 in a sensible way. They are used as numerical test beds under realistic operating conditions and thus cover an area which is not accessible via experimental means within TRR 40. Furthermore, the system competence accumulated within the research area and its actors contributed substantially to recommendations and refined requirements for experiment design, orientation and in particular relevant boundary and operating conditions for numerous projects of other research areas.

6.1 Combustion and Heat Transfer

Detailed knowledge about the effect of injector fluid dynamics and geometry variations on axial wall heat loads distribution and in particular performance are essential for the design of the cooling system, i.e. cooling channel geometry, the necessity for additional cooling methods such as film or transpiration cooling or thermal barrier coatings. For the new propellant combination oxygen/methane, a broad data base has been established for a wide range of combustion chamber pressures, propellant mixture ratios with different combustor applications having 1, 5 and 7 injector ele-
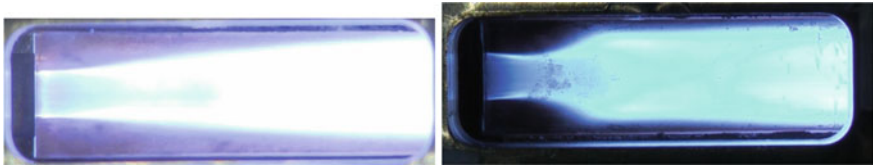
Fig. 21 Near-injector flame of a gas/gas (left) and gas/liquid (right) CH4/O2 Combustor
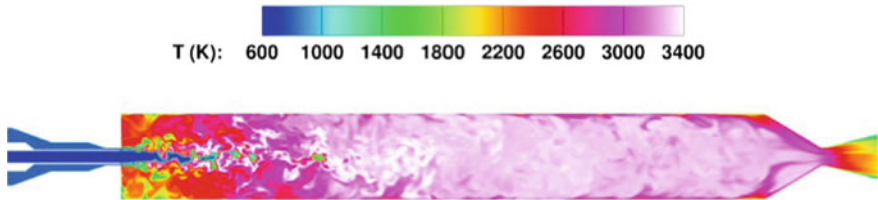

Fig. 22 Instantaneous temperature distribution for the PennState model combustor using iDDES

ments [52, 53]. Recently, the facility, a single injector combustor and the 7-injector element combustor were modified to allow for operation with liquid oxygen, too. Figure 21 shows the distinct differences of the near-injector regions of the single-injector flame for the cases of liquid and gaseous oxygen supply. Due to the much denser oxygen, the velocity ratio of these two cases with a mixture ratio of 2.6 and a combustion pressure of 20 bar, was 1.1 and 25.5, respectively. While the flame of the gas/gas case seems to expand at an almost constant angle, the flame of the liquid/gas case converges first but at a downstream position of one LOX jet diameter expands rather quickly. This is an effect which can be attributed to the very high momentum of the co-flowing methane.

A considerable effort has been made towards the development and validation of predictive tools which are sufficiently accurate but still require an acceptable numerical effort. The main emphasis was laid on models for chemical kinetics and turbulence, and in particular turbulence/chemistry interaction [54, 55]. One frequently simulated test case was the PennState preburner combustor [56], see Fig. 22, which has been simulated with a newly developed hybrid finite volume/transported PDF (TPDF) method. This revealed that near the faceplate a non-equilibrium chemistry approach is favorable [57]. A comparison of measured and simulated wall pressure and heat-flux distributions applying an adiabatic and a non-adiabatic flamelet approach revealed that although the overall trend of axial heat release was captured by both methods, the absolute values of pressure and heat flux differ from one another and from the experiments, too. While the non-adiabatic approach over-predicts the heat flux at a downstream position of 200 mm by about 40%, the adiabatic flamelet simulation yielded results similar to the experiment. Pressures however were under-predicted by 5% and 3%, respectively; see Fig. 23. Full-scale cases often consist of more than 100 injection elements with propellants injected at sub- or super-critical conditions. The latter requires different modeling strategies, namely the inclusion of
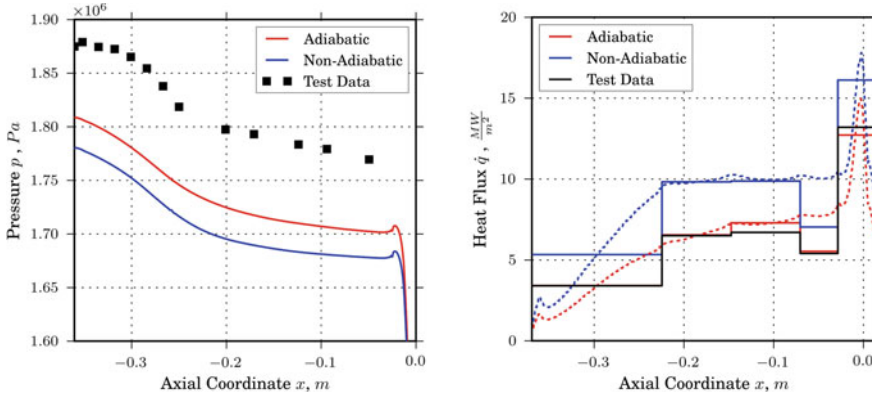
Fig. 23 Comparisons of measured and predicted wall pressure (left) and heat-flux (right) distributions
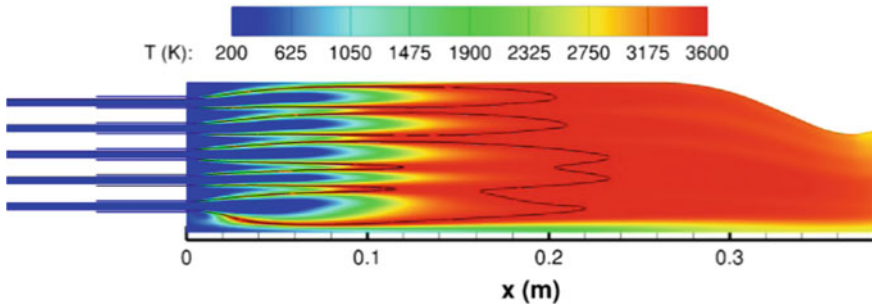

Fig. 24 Temperature distribution for TCD1 of project TP K4 using RANS. Black line indicates stoichiometric mixture fraction

a spray code and application of a real-gas equation of state. Such simulations were also performed, see Fig. 24 which depicts the predicted temperature distribution in the central in a plane of the Thrust Chamber Demonstrator (TCD1) of project K4 [58].

6.2   Dual Bell Nozzle

Experimental and numerical investigation of dual bell nozzles have been the key focus of project K2 (see Génin et al. in this volume). Previous investigations revealed that flow separation transition can be influenced not only by the variation of total propellant mass-flow rate but by a variation of the propellant mixture ratio r_{of} as well. While its increase yielded in a reduction of the transition pressure ratio, lowering of r_{of} produces an opposite result [59, 60]. However, these effects are accompanied by a reduction of the width of the hysteresis, the pressure ratio gap between transition
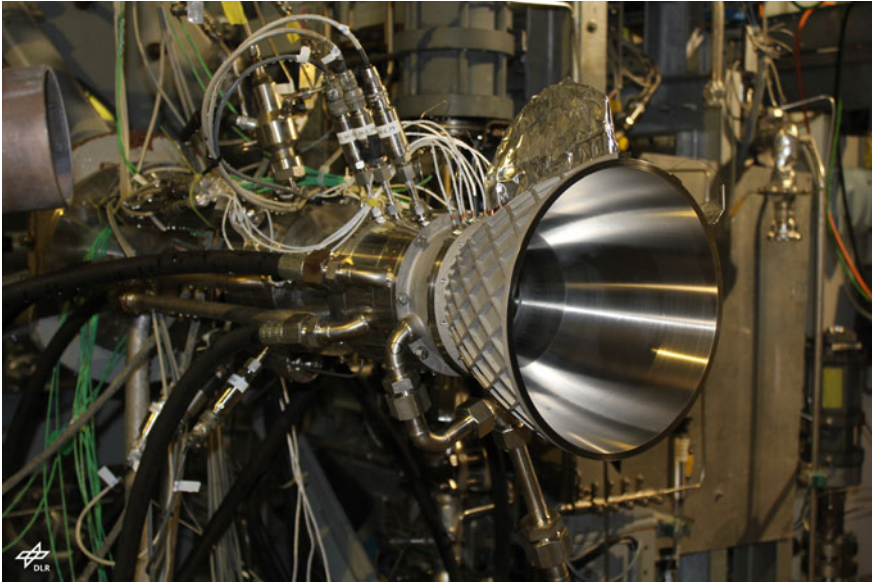
Fig. 25 Additive manufactured, film-cooled dual-bell nozzle at P8 test facility

and re-transition occurs. This effect is reducing the margin of stable operation in one particular mode in the presence of minor pressure and flow fluctuations around the nozzle. Recently, K2 put the focus on a combination of a classical convective cooled base nozzle and a film cooled nozzle extension with a dual-bell contour which was tested at DLR test facility P8, see Fig. 25. the operation with LOX/GH2 was tested in a subscale combustion chamber, equipped with a GH2 film cooled dual-bell nozzle [61].

6.3 Thrust-Chamber Demonstrators

ArianeGroup as a major European actor in space transportation activities has been involved in the TRR40 from the very beginning supporting the activities with its expertise and through contributions to the combustion modeling workshops of the summer program. ArianeGroup thus provided an industrial benchmark for the high-fidelity modeling approaches. In the final program period, ArianeGroup contributed and fully funded project K4 (see Eiringhaus et al. in this volume) to define virtual thrust-chamber demonstrators which covered all technical fields investigated within TRR40 and served as numerical test cases. As the design of a thrust chamber depends highly on its application, i.e. main or upper stage, and the chosen engine cycle, e.g. gas generator or expander cycle, not all relevant design features can be covered by a single demonstrator and therefore three different concepts were defined [62]. They have
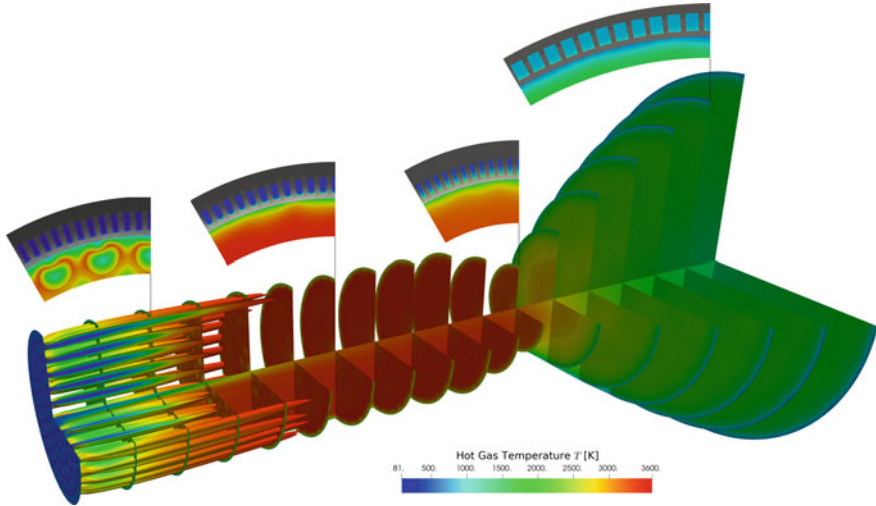
Fig. 26 Hot-gas temperature field of demonstrator TCD1 illustrated at several axial and lateral slices as well as for the stoichiometric mixture surface. Additional axial slices at selected positions display the strong temperature gradients to be resolved in the structure

been used as well for the continuous maturation of the in-house tool Rocflam3. As already mentioned, Rocflam3 has been extended with a new conjugate heat transfer (CHT) environment for fully 3D analyses of full-scale liquid rocket combustion chambers unique within the TRR40. The resulting hot-gas temperature field as well as selected axial slices of the structure and coolant temperatures of such a CHT simulation of demonstrator TCD1 are illustrated in Fig. 26. Further investigations show a circumferential wall temperature stratification stemming from a superposition of injection pattern as well as cooling channel effects. These variations reach up to 100 K on the hot-gas wall [58]. Additionally, the individual cooling channels show only minor variances in coolant heat up and pressure loss, making this stratification difficult to detect in full-scale experiments.

7 Central Research and Education Support

Cooperation within TRR40 as well as with people and entities outside the center employed several instruments, ranging from individually arranged working-group meetings, weekly seminars with national and international experts, graduate education and summer research programs to frequent and regular bi-annual, or quarterly, research area meetings. Meetings of project groups at the TRR40 sites allowed doctoral students to acquire knowledge from across the different divisions and to establish new and improve existing collaborations.

A particular event of TRR40 was the biennual summer program with the main objective to establish cooperation between visiting scientists (preferably early post-docs or experienced doctoral students) and members of TRR40 project groups. The number of working teams grew from 11 in 2011 to 15–20 in the past years with participation of 20–30 visiting scientists from up to 9 different countries. Special lectures for the summer program on launcher-related topics have been delivered in the course of the summer program. The projects reports can be found in the four summer-program volumes [63–67].

A combustion modelling workshop was integrated into the 2015, 2017 and 2019 summer programs, where the project K1 provided test cases [68, 69] and a reference reaction mechanism [70] to foster competitive numerical comparison with experimental heat transfer and pressure data. In addition to TRR40 members, participants from universities, research labs, agencies and industry took up the challenge and generated valuable data for the evaluation and improvement of their numerical methods.

The special education for PhD students within the TRR40 took place locally for the different universities and research institutions involved. Annually, the PhD students and interested researchers in the field of rocket propulsion and related topics were invited to a week-long seminar exposing them to challenges of current launcher technologies brought forth by international experts in the field. Material science, combustion modelling, thermodynamics, computational fluid dynamics are just a few of the focal points of these graduate seminars. During the course of the involvement with the TRR40, the PhD students had to spend at least 4 weeks abroad or with an industrial partner. Most students took advantage of this unique opportunity and went abroad for 2–3 months which helped to establish a scientific network as well as towards an international visibility of the program itself. As a service task to all the projects involved, the TRR40 has undergone a rigorous evaluation of the turbulence modelling activities involved in the computational fluid-dynamic projects. The outcome has been documented in a best-practice guide [71] for all groups to ensure comparability and transferability of the results from within the TRR40.

References

1. Lasheras, J.C., Hopfinger E.J.: Liquid jet instability and atomization in a coaxial gas stream. In: Annual Review of Fluid Mechanics, vol. 32, 2000, pp. 275–308 (2000). ISBN 0-8243-0732-1
2. Yang, V., Anderson, W. (eds.): Liquid Rocket Engine Combustion Instability, Progress in Astronautics and Aeronautics, vol. 169, AIAA (1995). ISBN 1-56347-183-3
3. Popp. M., Hulka, J., Yang, V., Habiballah, M. (eds.): Liquid Rocket Thrust Chambers: Aspects of Modeling, Analysis and Design, Progress in Astronautics and Aeronautics, vol. 200, AIAA (2004). ISBN 978-1-56347-223-7
4. Haidn, O.J.: Advanced Rocket Engines, in Advances in Propulsion Technology for High-Speed Aircraft, RTO-EN-AVT-150, RTO/NATO, pp. 6.1–6.40 (2007). ISBN 978-92-837-0085
5. Sutton, G.P., Biblarz, O.: Rocket Propulsion Elements, 9th edn. Wiley, New York (2016)
6. Huzel, D.K., Huang, D.: Modern Engineering for Design of Liquid-Propellant Rocket Engines, AIAA (1992). ISBN 978-1-56347-013-6

7. Dahmen, W., et al.: Numerical boundary layer investigations of transpiration-cooled turbulent channel flow. Int. J. Heat Mass Transf. **86**, 90–100 (2015). https://doi.org/10.1016/j.ijheatmasstransfer.2015.02.075

8. Herty, M., Müller, S., Gerhard, S.N., Xiang, G., Wang, B.: Fluid-structure coupling of linear elastic model with compressible flow models. Int. J. Numer. Methods Fluids **86**(6), 365–391 (2018). https://doi.org/10.1002/fld.4422

9. König, V., et al.: Numerical and experimental investigation of transpiration cooling with C/C characteristic outflow distributions. J. Thermophys. Heat Transf. (2018). https://doi.org/10.2514/1.T5457

10. Deolmi, G., et al.: Effective boundary conditions: a general strategy and application to compressible flows over rough boundaries. Commun. Comput. Phys. **21**(2), 358–400 (2017)

11. Schweikert, S., et al.: Characterization of actively cooled porous C/C wall segments according to pressure loss and internal temperature distribution. In: 7th European Workshop on Thermal Protection Systems & Hot Structures, Noordwijk (2013)

12. Dittert, C., et al.: Flowfield and pressure decay analysis of porous cones. AIAA J. **55**(3), 874–882 (2017). https://doi.org/10.2514/1.J055298

13. Yahiaoui, G., Olivier, H.: Development of a short-duration rocket nozzle flow simulation facility. AIAA J. **53**(9), 2713–2725 (2015). https://doi.org/10.2514/1.J053790

14. Ludescher, S., Olivier, H.: Experimental investigations of film cooling in a conical nozzle under rocket-engine-like flow conditions. AIAA J. **57**(3), 1172–1183 (2019). https://doi.org/10.2514/1.J057486

15. Peter, J.M.F., Kloker, M.J.: Direct numerical simulation of supersonic film cooling by tangential blowing. In: Nagel, W.E., Kröner, , D.B., Resch, M.M. (eds.) Transactions of the HLRS High Performance Computing in Science and Engineering '19, 17 pages, Springer (2019). https://doi.org/10.1007/978-3-03x

16. Christopher, N., et al.: DNS of Turbulent Flat-Plate Flow with Transpiration Cooling, accepted by International Journal Heat Fluid Flow

17. van Buren, S., et al.: Large Eddy simulation of enhanced heat transfer in pulsatile turbulent channel flow. Int. J. Heat Mass Transf. **144**, 118585 (2019). https://doi.org/10.1016/j.665ijheatmasstransfer.2019.118585

18. Scharnowski, S., Bolgar, I., Kähler, C.J.: Characterization of turbulent structures in a transonic backward-facing step flow. Flow, Turbul. Combust. **98**(4), 947–967 (2017)

19. Bolgar, I., Scharnowski, S., Kähler, C.J.: The effect of the Mach number on a turbulent backward-facing step flow. Flow, Turbul. Combust. **101**(3), 653–680 (2018)

20. Stephan, S., Radespiel, R.: Propulsive jet simulation with air and helium in launcher wake flows. CEAS Space J. **14**(3), 394 (2016)

21. Barklage, A., Loosen, S., Schröder, W., Radespiel, R.: Reynolds number influence on the hysteresis behavior of a dual-bell nozzle. In: Proceedings of the 8th European Conference for Aerospace Sciences (EUCASS), EUCASS2019-519 (2019)

22. Saile, D., Kühl, V., Gülhan, A.: On the subsonic near-wake of a space launcher configuration with exhaust jet. Exp. Fluids **60**(165), 17 (2019)

23. Kirchheck, D., Saile, D., Gülhan, A.: Spectral analysis of rocket wake flow-jet interaction by means of high-speed schlieren imaging. In: Proceedings of the 8th European Conference for Aerospace Sciences (EUCASS), EUCASS2019-1057 (2019)

24. Statnikov, V., Meinke, M., Schröder, W.: Reduced-order analysis of buffet flow of space launchers. J. Fluid Mech. **815**, 1–25 (2017)

25. Loosen, S., Meinke, M., Schröder, W.: Numerical investigation of jet-wake interaction for a dual-bell nozzle. Flow Turbul. Combust. **104**(2), 553–578 (2020)

26. Horchler, T., Oßwald, K., Hannemann, V., Hannemann, K.: Hybrid RANS-LES study of transonic flow in the wake of a generic space launch vehicle. In: Progress in Hybrid RANS-LES Modelling, vol. 137, pp. 291–300 (2018)

27. Schumann, J.-E., Hannemann, V., Hannemann, K.: Investigation of structured and unstructured grid topology and resolution dependence for scale-resolving simulations of axisymmetric detaching-reattaching shear layers. In: Progress in Hybrid RANS-LES Modelling, vol. 143, pp. 169–179 (2020)

28. Lamanna, G., et al.: On the importance of non-equilibrium models for describing coupling of heat and mass transfer at high pressure. Int. Commun. Heat Mass Transf. **96**, 49–58 (2018). https://doi.org/10.1016/j.cheatmasstransfer.2018.07.012
29. Openfoam 4.1. https://openfoam.org/
30. Traxinger, C., et al.: A pressure-based solution framework for sub-and supersonic flows considering real-gas effects and phase separation under engine-relevant conditions. In: Computers & Fluids, in press, (2020)
31. Traxinger, C., et al.: Single-phase instability in non-premixed flames under liquid rocket engine relevant conditions. J. Propuls. Power **35**(4), 675–689 (2019)
32. Traxinger, C., et al.: Experimental and numerical investigation of phase separation due to multi-component mixing at high-pressure conditions. Phys. Rev. Fluids **4**(7), 074303 (2019)
33. Zips, J., et al.: Assessment of presumed/transported probability density function methods for rocket combustion chambers. J. Propuls. Power (2019). https://doi.org/10.2514/1.B37331
34. Celano, M.P., et al.: Gaseous film cooling investigation in a model single element GCH4-GOX combustion chamber. Trans. JSASS Aerospace Tech. Japan. **14**, 129–137 (2016)
35. Egerer, C.P., et al.: Efficient implicit LES method for the simulation of turbulent cavitating flows. J. Comput. Phys. **316**, 453–469 (2016)
36. MacDonald, M., et al.: Direct numerical simulation of high aspect ratio spanwise-aligned bars. J. Fluid Mech. **843**, 422–432 (2018)
37. Sattelmayer, T., et al.: Interaction of combustion with transverse velocity fluctuations in liquid rocket engines. J. Propuls. Power **31**(4), 1137–1147 (2015)
38. Schulze, M., Sattelmayer, T.: Linear stability assessment of a cryogenic rocket engine. Int. J. Spray Combus. Dyn. **9**(4), 277–298 (2017)
39. Chemnitz, A., Sattelmayer, T.: Influence of radial stratification on eigenfrequency computations in rocket combustion chambers. In: 8th EUCASS (2019)
40. Sattelmayer, T., et al.: Validation of transverse instability damping computations for rocket engines. J. Propuls. Power **31**(4), 1148–1158 (2015)
41. Chemnitz, A., et al.: Modification of eigenmodes in a cold-flow rocket combustion chamber by acoustic resonators, J. Propuls. Power **35**(4) (2019)
42. Gröning, S., et al.: Injector-driven combustion instabilities in a Hydrogen/Oxygen rocket combustor. J. Propuls. Power **32**(3), 560–573 (2016). https://doi.org/10.2514/1.B35768
43. Nez, R., et al.: High-frequency combustion instabilities in liquid rocket engines driven by propellants flow rate oscillations. Space Propulsion, Madrid (2018)
44. Urbano, A., et al.: Analysis of coaxial-flame response during transverse combustion instability. In: 7th EUCASS, Milano (2017). https://doi.org/10.13009/EUCASS2017-609
45. Fassin, M.: Gradient-extended anisotropic brittle damage modeling using a second order damage tensor - Theory, implementation and numerical examples. Int. J. Solids Struct. **167**, 93–126 (2019). https://doi.org/10.1016/j.ijsolstr.2019.02.009
46. Fassin, M., et al.: Design studies of rocket engine cooling structures for fatigue experiments, Archive of Applied Mechanics, vol. 86 (12), 2063–2093 (2016). ISSN: 0939-1533, https://doi.org/10.1007/s00419-016-1160-6
47. Fiedler, T., et al.: A new metallic thermal Barrier coating System for Rocket Engines: Failure Mechanisms and Design Guidelines. J. Therm. Spray Technol. **28**, 1402–1419 (2019)
48. Fiedler, T., et al.: Damage mechanisms of metallic HVOF-coatings for high heat flux application. Surf. Coat. Technol. **316**, 219–225 (2017)
49. Rochlitz, H., et al.: The flow field in a high aspect ratio cooling duct with and without one heated wall. Exp. Fluids **56**(12), 1–13 (2015)
50. Kaller, T., et al.: Turbulent flow through a high aspect ratio cooling duct with asymmetric wall heating. J. Fluid Mech. **860**, 258–299 (2019)
51. Daub, D., et al.: Experiments on high temperature hypersonic fluid-structure interaction with plastic deformation. AIAA Journal (in press) (2020)
52. Celano, M.P., et al.: Comparison of a single and multi-injector GOX/GCH4 Combustion Chamber. In: 52nd AIAA Joint Propulsion Conference (2016). https://doi.org/10.2514/6.2016-49902016

53. Perakis, N., et al.: Heat transfer and combustion simulation of a 7-element GOX/GCH4 rocket combustor. J. Propuls. Power **35**(6) (2019). https://doi.org/10.2514/1.B37402
54. Maestro, D., et al.: Numerical investigation of flow and combustion in a single-element GCH4/GOX rocket combustor: chemistry modeling and turbulence/combustion interaction. In: 52nd Joint Propulsion Conference (2016)
55. Chemnitz, A., et al.: Numerical investigation of flow and combustion in a single-element GCH4/GOX rocket combustor: aspects of turbulence modeling. J. Propuls. Power **34**, 864–877 (2018). https://doi.org/10.2514/1.B36565
56. Marshall, M., et al.: Benchmark wall heat flux data for a GO2/GH2 single element combustor. In: 41^{s}t AIAA-2005-3572 (2005). https://doi.org/10.2514/6.2005-3572
57. Gerlinger, P.: Lagrangian transported MDF methods for compressible high speed flows. J. Comput. Phys. **339**, 68–95 (2017). https://doi.org/10.1016/j.jcp.2017.02.049
58. Eiringhaus, D., et al.: 3D conjugate heat transfer analysis of a 100 kN class liquid rocket combustion chamber. In: 8^{t}h European Conference for Aeronautics and Space Sciences (EUCASS), Madrid (2019). https://doi.org/10.13009/EUCASS2019-251
59. Génin, C., et al.: LOX/CH4 Hot Fire Dual Bell Nozzle Testing: Part 1-Transitional Behavior, AIAA paper 2015-4155, https://doi.org/10.2514/6.2015-4155
60. Schneider, D., et al.: A Numerical Model for Nozzle Flow Application under LOX/CH4 Hot Flow Condition, AIAA, paper 2016-4671. https://doi.org/10.2514/6.2016-4671
61. Schneider, D., et al.: Active control of dual-bell nozzle operation mode transition by film-cooling and mixture ratio variation. J. Propuls. Power **36**(1), 47–58 (2020). https://doi.org/10.2514/1.B37299
62. Eilringhaus, et al.: Full-Scale Virtual Thrust Chamber Demonstrators as Numerical Testbeds within SFB-TRR 40, AIAA 2018-4469 (2018). https://doi.org/10.2514/6.2018-4469
63. Stemmer, C., et al.: SFB/TRR 40 Summer Program, Technische Universität München (2011)
64. Stemmer, C., et al.: SFB/TRR 40 Summer Program, Technische Universität München (2013)
65. Stemmer, C., et al.: SFB/TRR 40 Summer Program, Technische Universität München (2015)
66. Stemmer, C., et al.: SFB/TRR 40 Summer Program, Technische Universität München (2017)
67. Stemmer, C., et al.: SFB/TRR 40 Summer Program, Technische Universität München (2019)
68. Haidn, O.J., et al.: Test Case 1: Single Element Combustion Chamber - GCH4 / GOX. http://www.sfbtr40.de/index.php?id=summerprogram2015
69. Haidn, O.J., et al.: Test Case BKS-2: 7-Element Combustion Chamber - GCH4 / GOX. http://www.sfbtr40.de/index.php?id=summerprogram2017
70. Slavinskaya, N.A., et al.: Skeletal Mechanism of Methane Oxidation for Space Applications, AIAA-2016-4781 (2016)
71. Adams, N.A., et al.: Best Practice Guidelines for Turbulence Modeling in Rocket Propulsion (2015). http://www.sfbtr40.de/index.php?id=bpgturbulencemodeling